

## Constraining the Higgs boson self-coupling in a combined measurement of single and double Higgs boson channels at the ATLAS experiment

---

Valerio D'Amico on behalf of the ATLAS Collaboration<sup>a,\*</sup>

<sup>a</sup>*Ludwig-Maximilians-Universität München,  
Am Coulombwall 1, Garching, Deutschland*

*E-mail:* [valerio.damico@cern.ch](mailto:valerio.damico@cern.ch)

The most precise measurements of single and double Higgs boson production cross sections are obtained from a combination of measurements performed in different Higgs boson production and decay channels. While double Higgs production can be used to directly constrain the Higgs boson self-coupling, this parameter can be also constrained by exploiting higher-order electroweak corrections to single Higgs boson production. A combined measurement of both results yields the overall highest precision, and reduces model dependence by allowing for the simultaneous determination of the single Higgs boson couplings. Results for this combined measurement are presented based on  $pp$  collision data collected at a centre-of-mass energy of 13 TeV with the ATLAS detector.

*41st International Conference on High Energy physics - ICHEP2022  
6-13 July, 2022  
Bologna, Italy*

---

\*Speaker

## 1. Introduction

After the discovery of the Higgs boson by the ATLAS [1, 2] and CMS Collaborations [3, 4] at the Large Hadron Collider (LHC), the measurement of its properties has become of major importance for the physics program of the LHC experiments in order to verify their compatibility with the prediction of the Standard Model (SM) of particle physics. One of the most important features of the Higgs boson is its self-interaction, characterised by the trilinear self-coupling  $\lambda_{HHH}$ , and related to the shape of the Higgs potential [5–7]. This property influences the SM prediction of the non-resonant Higgs boson pair ( $HH$ ) production cross-section. The observation of this process will be able to test the SM description of the Englert-Brout-Higgs mechanism and provide a measurement of the Higgs boson self-coupling value. Results on Higgs boson self-coupling are usually expressed using the kappa-framework coupling modifier  $\kappa_\lambda = \lambda_{HHH}/\lambda_{HHH}^{SM}$ .  $HH$  production is directly sensitive to the Higgs boson self-coupling starting at the lowest order in perturbation theory. In the SM, the gluon-gluon fusion process (ggF  $HH$ ) accounts for more than 90% of the  $pp \rightarrow HH$  cross-section, while the second most abundant process is the VBF  $HH$  production, accounting for only 5% of the total  $HH$  production. Feynman diagram examples of these two production modes are shown in Figure 1, where the coupling modifiers accessible via each diagram are highlighted.

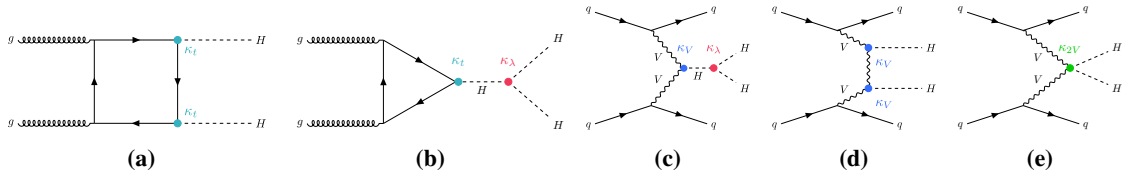


**Figure 1:** Examples of leading-order Feynman diagrams for Higgs boson pair production for ggF mode (a,b), and VBF mode (c,d,e). The Higgs coupling modifiers are also shown for the HHVV ( $\kappa_{2V}$ ), HVV ( $\kappa_V$ ), Higgs self-coupling ( $\kappa_\lambda$ ), and top quark Yukawa coupling modifier ( $\kappa_t$ ). [20].

Single-Higgs processes are indirectly sensitive to  $\kappa_\lambda$  via next-to-leading-order (NLO) electroweak (EW) corrections. A universal correction of  $O(\kappa_\lambda^2)$  is possible through Higgs loops, as visible from Figure 2(a), while linear corrections of the order of  $O(\kappa_\lambda)$  are process and kinematic dependent, as visible from Figure 2(b,c,d,e). As a result, production cross sections and branching ratios vary as a function of  $\kappa_\lambda$  [8, 9], and precise measurements of inclusive and differential single-Higgs production cross sections and decays provide indirect constraints on  $\kappa_\lambda$ .

In this work the combination of the three most sensitive double-Higgs decay channels,  $b\bar{b}\gamma\gamma$  [10],  $b\bar{b}\tau\tau$  [11], and  $b\bar{b}b\bar{b}$  [12], using the dataset collected by ATLAS at  $\sqrt{s} = 13$  TeV between 2015 and 2018, corresponding to an integrated luminosity of 126-139  $\text{fb}^{-1}$ , is reported. This combination is used to set constraints on the  $HH$  production cross-section and on  $\kappa_\lambda$ . More stringent constraints on  $\kappa_\lambda$  are also reported, from the combination of  $HH$  results with the combination of recent single-Higgs analyses in the  $\gamma\gamma$ ,  $ZZ^*$ ,  $\tau^+\tau^-$ ,  $WW^*$ , and  $b\bar{b}$  [13–19] decay channels at ATLAS. The single-Higgs measurements of the simplified template cross-sections (STXS) and the  $HH$  results have been parameterised to take into account the impact of  $\kappa_\lambda$  and the other coupling modifiers. This combination allows to measure  $\kappa_\lambda$ , relaxing the assumptions on the Higgs boson interactions with the other SM particles, thus obtaining a less model dependent result.

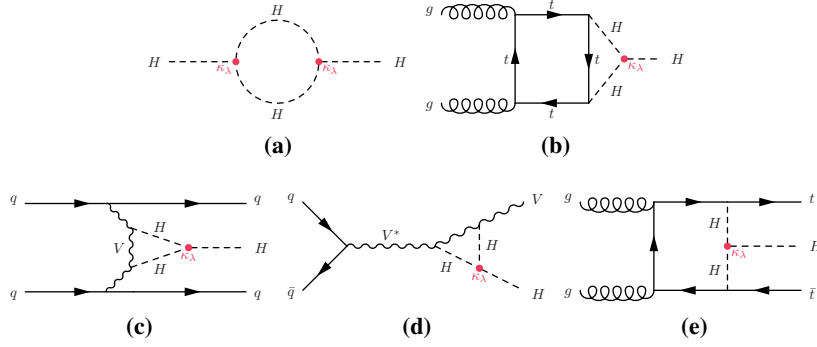


**Figure 2:** Examples of one loop  $\kappa_\lambda$ -dependent diagrams for the Higgs boson self-energy (a) and the single-Higgs production in the ggF (b), VBF (c),  $VH$  (d), and  $ttH$  (e) modes [20].

## 2. Statistical model

The parameterisation of ggF  $HH$  production is provided generating the signal samples at different values of  $\kappa_\lambda$ , and for the VBF production also  $\kappa_V$  and  $\kappa_{2V}$ . The inclusive production cross-sections, decay branching ratios and differential cross-sections are exploited to increase the sensitivity of the single-Higgs analyses to  $\kappa_\lambda$  and the other coupling modifiers  $\kappa_m$ . The differential information of single-Higgs analyses is encoded in the STXS framework, with a signal yield in a specific decay channel and STXS bin being proportional to:

$$n_{i,f}^{\text{signal}}(\kappa_\lambda, \kappa_m) \propto \mu_i(\kappa_\lambda, \kappa_m) \times \mu_f(\kappa_\lambda, \kappa_m) \times \sigma_{\text{SM},i} \times \text{BR}_{\text{SM},f} \times (\varepsilon \times A)_{i,f} \quad (1)$$

where  $\mu_i$  and  $\mu_f$  describe respectively the multiplicative corrections of the expected SM Higgs boson production cross-sections in an STXS bin ( $\sigma_{\text{SM},i}$ ) and each decay-channel branching ratio ( $\text{BR}_{\text{SM},f}$ ), as a function of the values of  $\kappa_\lambda$  and  $\kappa_m$ . The  $(\varepsilon \times A)_{i,f}$  coefficients take into account the analysis efficiency times acceptance in each production and decay mode. The results are obtained from a likelihood function, with the systematic uncertainties and background parameters that are constrained by sidebands or control regions in data treated as nuisance parameters. The global likelihood function is obtained as the product of the likelihoods of each input analysis, which are products of likelihoods computed in the single analysis categories as well. The results presented here are based on the profile likelihood ratio test statistic  $\Lambda$ , and 68% as well as 95% confidence level (CL) intervals are derived in the asymptotic approximation. The detailed discussion of the sources of systematic uncertainty implemented in the individual analyses is described in Ref. [10–19], and the correlation model adopted for the systematic uncertainties within the single-Higgs combination is described in detail in Ref. [21]. The additional correlation of systematic uncertainties between  $HH$  analyses and between the single-Higgs and  $HH$  combination has been investigated and implemented, and are described in detail in Ref. [20].

## 3. Double-Higgs analyses combination results

The double-Higgs boson analyses are combined in order to extract constraints on the production cross-section and on the Higgs-boson self-coupling. The value of the signal strength  $\mu_{HH}$ , defined as the  $HH$  cross-section, only including the ggF  $HH$  and VBF  $HH$  processes, normalised to its

SM prediction, is determined. This combination yields an observed (expected) upper limit on  $\mu_{HH}$  of 2.4 (2.9) at 95% CL assuming no  $HH$  production. The limits on the  $\mu_{HH}$  obtained from the individual channels and their combination are shown in Figure 3(a). The best fit value obtained from the fit to the data is  $\mu_{HH} = -0.73 \pm 1.25$ , which is compatible with the SM prediction of unity with a p-value of 0.2. The observed (expected) limit can be translated into an upper limit on  $\sigma(pp \rightarrow HH)$  of 73 fb (85 fb) at 95% CL, assuming no  $HH$  production. The cross-section limit as a function of  $\kappa_\lambda$  is shown in Figure 3(b), exhibiting a strong dependence of the  $HH$  signal acceptance on  $\kappa_\lambda$ . The combined  $HH$  channels are also sensitive to the VBF  $HH$  process and to the  $HHVV$  quartic interaction, and the 95% CL observed VBF  $HH$  cross-section upper limit as a function of  $\kappa_{2V}$  is shown in Figure 3(c).

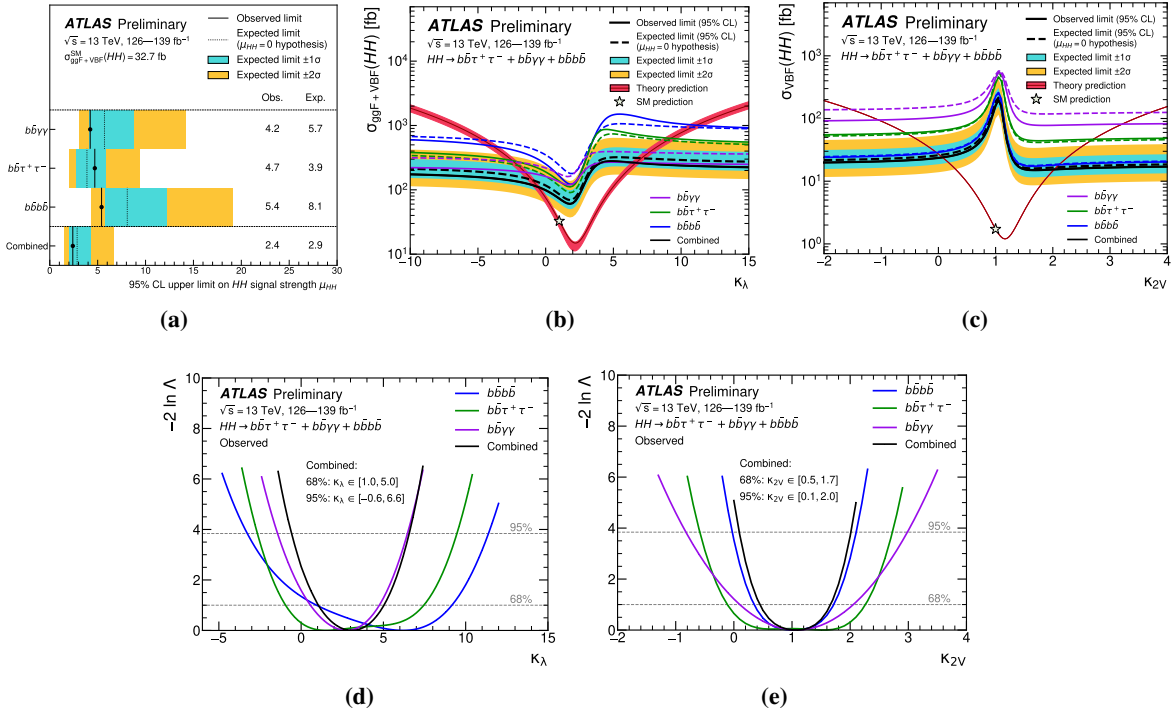


**Figure 3:** Observed and expected 95% CL upper limits on  $\mu_{HH}$  from the three double-Higgs search channels, and their combination (a). Observed and expected 95% CL exclusion limits on the production cross-sections of (b) the combined ggF  $HH$  and VBF  $HH$  as a function of  $\kappa_\lambda$  and (c) the VBF  $HH$  process as a function of  $\kappa_{2V}$ , for the three  $HH$  search channels and their combination. The expected limits assume no  $HH$  production (a,b) or no VBF  $HH$  production (c). The red line shows the theory prediction for (b) the combined ggF  $HH$  and VBF  $HH$  cross-section as a function of  $\kappa_\lambda$ , and (c) the VBF  $HH$  cross-section as a function of  $\kappa_{2V}$ , with the surrounding band indicating the theoretical uncertainty on the predicted cross-section. Observed value of the test statistic ( $-2 \ln \Lambda$ ), as a function of the  $\kappa_\lambda$  (d), and  $\kappa_{2V}$  (e) parameter for the three  $HH$  search channels and their combination, where all other coupling modifiers are fixed to their SM value [20].

Constraints on the coupling modifiers are obtained by using the values of the test statistic  $-2 \ln \Lambda$  as a function of  $\kappa_\lambda$  and  $\kappa_{2V}$ , shown in Figure 3(d,e), in the asymptotic approximation and including the theoretical uncertainty on the cross-section predictions. The observed (expected) constraints at 95% CL are  $-0.6 < \kappa_\lambda < 6.6$  ( $-2.1 < \kappa_\lambda < 7.8$ ), and  $0.1 < \kappa_{2V} < 2.0$  ( $0.0 < \kappa_{2V} < 2.1$ ), with the expected values derived under the SM hypothesis.

#### 4. Single- and double-Higgs analyses combination results

The  $HH$  and single-Higgs analyses are combined to derive constraints on  $\kappa_\lambda$ . Several fits to data are performed with different assumptions on the Higgs coupling modifiers, summarised in Table 1. Considering only possible deviations from the SM of  $\kappa_\lambda$  and assuming that all other Higgs boson interactions proceed as predicted by the SM, the observed values of the test statistic  $-2 \ln \Lambda$  as a function of  $\kappa_\lambda$  are obtained and shown in Figure 4(a) for the single-Higgs,  $HH$  analyses, and their combination. The combined observed (expected) constraints obtained under this hypothesis are  $-0.4 < \kappa_\lambda < 6.3$  ( $-1.9 < \kappa_\lambda < 7.5$ ) at 95% CL. The addition of the single-Higgs analyses gives the possibility to relax assumptions on the coupling modifiers to other SM particles. Removing the assumption on the coupling modifier  $\kappa_t$  between the Higgs and the top quark, and allowing it to float freely in the fit, allows to obtain the two dimensional contours of the test statistic in the  $\kappa_\lambda - \kappa_t$  plane. These contour plots are shown in Figure 4(b,c), fixing all the other coupling modifiers to unity. Thanks to the strong constraints on  $\kappa_t$  from single-Higgs measurements visible in the contour plots, the constraints on  $\kappa_\lambda$  obtained from a fit with a free floating value of  $\kappa_t$  are similar to those obtained with its value fixed to unity, as reported in Table 1.

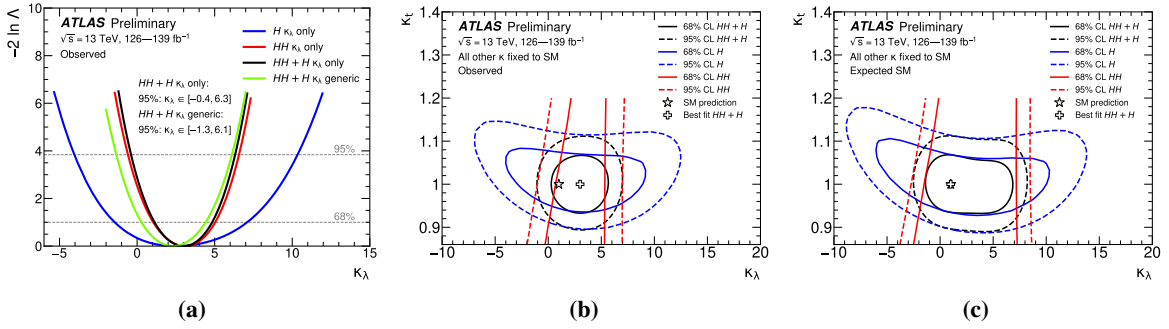


**Figure 4:** Observed value of the test statistic ( $-2 \ln \Lambda$ ) as a function of  $\kappa_\lambda$  (a), and observed (b) and expected (c) constraints in the  $\kappa_\lambda - \kappa_t$  plane, from single-Higgs (blue),  $HH$  (red) and their combination (black). The combined result for the generic model is also shown in (a) (green curve) [20].

| Combination assumption  | Obs. 95% CL                    | Exp. 95% CL                    | Obs. value $^{+1\sigma}_{-1\sigma}$  |
|---|--------------------------------|--------------------------------|--------------------------------------|
| $HH$ combination  | $-0.6 < \kappa_\lambda < 6.6$  | $-2.1 < \kappa_\lambda < 7.8$  | $\kappa_\lambda = 3.1^{+1.9}_{-2.0}$ |
| Single- $H$ combination   | $-4.0 < \kappa_\lambda < 10.3$ | $-5.2 < \kappa_\lambda < 11.5$ | $\kappa_\lambda = 2.5^{+4.6}_{-3.9}$ |
| $HH$ +Single- $H$ combination   | $-0.4 < \kappa_\lambda < 6.3$  | $-1.9 < \kappa_\lambda < 7.6$  | $\kappa_\lambda = 3.0^{+1.8}_{-1.9}$ |
| $HH$ +Single- $H$ combination, $\kappa_t$ floating                                  | $-0.4 < \kappa_\lambda < 6.3$  | $-1.9 < \kappa_\lambda < 7.6$  | $\kappa_\lambda = 3.0^{+1.8}_{-1.9}$ |
| $HH$ +Single- $H$ combination, $\kappa_t, \kappa_V, \kappa_b, \kappa_\tau$ floating | $-1.4 < \kappa_\lambda < 6.1$  | $-2.2 < \kappa_\lambda < 7.7$  | $\kappa_\lambda = 2.3^{+2.1}_{-2.0}$ |

**Table 1:** Summary of  $\kappa_\lambda$  observed and expected constraints and corresponding observed best fit values with their uncertainties for different combination assumptions [20].

The most generic model allows all coupling modifiers implemented in this parameterisation,  $\kappa_\lambda$ ,  $\kappa_t$ ,  $\kappa_b$ ,  $\kappa_\tau$ , and  $\kappa_V$ , to freely float in the fit, with the exception of  $\kappa_{2V}$  that is fixed to unity, since there is no available parameterisation of single-Higgs NLO EW correction as a function of this coupling modifier. In this combination, an observed (expected) exclusion of  $-1.3 < \kappa_\lambda < 6.1$  ( $-2.1 < \kappa_\lambda < 7.6$ ) is obtained at 95% CL in this less model-dependent fit. The post-fit values of all the other coupling modifiers are in agreement with the SM prediction within uncertainties.

## 5. Conclusions

The single-Higgs and double-Higgs boson analyses based on the full Run 2 LHC dataset collected with the ATLAS detector have been combined to investigate the Higgs boson self-interaction. Using the three most sensitive  $HH$  channels,  $b\bar{b}\gamma\gamma$ ,  $b\bar{b}\tau\tau$ , and  $b\bar{b}b\bar{b}$ , an observed (expected) upper limit of 2.4 (2.9) at 95% CL has been set on the  $HH$  signal strength, defined as the sum of the ggF  $HH$  and VBF  $HH$  production cross-sections normalised to its SM prediction. A constraint of  $-0.6 < \kappa_\lambda < 6.6$  at 95% CL on the Higgs boson self-coupling modifier has been set, assuming that the other Higgs boson interactions are as predicted by the SM. In addition, thanks to the sensitivity of the VBF  $HH$  process, a constraint of  $0.1 < \kappa_{2V} < 2.0$  at 95% CL on the  $\kappa_{2V}$  coupling modifier has been derived. The  $HH$  channels results have been combined with the single-Higgs boson cross-section measurements from the  $\gamma\gamma$ ,  $ZZ^*$ ,  $\tau^+\tau^-$ ,  $WW^*$ , and  $b\bar{b}$  decay channels, to derive less model dependent constraints on  $\kappa_\lambda$ . Using this combination and assuming that  $\kappa_\lambda$  is the only source of physics beyond the SM, an observed (expected) exclusion limit of  $-0.4 < \kappa_\lambda < 6.3$  ( $-1.9 < \kappa_\lambda < 7.5$ ) at 95% CL has been set. A less model-dependent result is obtained relaxing the assumptions on the other coupling modifiers,  $\kappa_t$ ,  $\kappa_b$ ,  $\kappa_\tau$ , and  $\kappa_V$ , with an observed (expected) constraint of  $-1.3 < \kappa_\lambda < 6.1$  ( $-2.1 < \kappa_\lambda < 7.6$ ) at 95% CL. To date, this study provides the most stringent constraints on the Higgs boson self-interactions.

## References

- [1] ATLAS Collaboration, 2008 JINST 3 S08003.
- [2] ATLAS Collaboration, Phys. Lett. B **716** (2012) 1.
- [3] CMS Collaboration, JINST, 3 (2008), S08004.
- [4] CMS Collaboration, Phys. Lett. B **716** (2012) 30.
- [5] F. Englert and R. Brout, Phys. Rev. Lett. **13** (1964) 321.
- [6] P. W. Higgs, Phys. Rev. Lett. **13** (1964) 508.
- [7] P. W. Higgs, Phys. Rev. **145** (1966) 1156.
- [8] G. Degrandi, P. Giardino, F. Maltoni *et al.*, J. High Energ. Phys. **2016**, 80 (2016).
- [9] F. Maltoni, D. Pagani, A. Shivaji and X. Zhao, Eur. Phys. J. C **77** (2017) no.12, 887.
- [10] ATLAS Collaboration, Phys. Rev. D **106**, 052001.
- [11] ATLAS Collaboration, arXiv:2209.10910.
- [12] ATLAS Collaboration, ATLAS-CONF-2022-035.
- [13] ATLAS Collaboration, arXiv:2207.00348.
- [14] ATLAS Collaboration, Eur. Phys. J. C **80**, 957 (2020).
- [15] ATLAS Collaboration, JHEP **08** (2022), 175.
- [16] ATLAS Collaboration, arXiv:2207.00338.
- [17] ATLAS Collaboration, Eur. Phys. J. C **81**, 178 (2021).
- [18] ATLAS Collaboration, Eur. Phys. J. C **81**, 537 (2021).
- [19] ATLAS Collaboration, JHEP **06** (2022), 097.
- [20] ATLAS Collaboration, ATLAS-CONF-2022-050.
- [21] ATLAS Collaboration, Nature **607**, 52–59 (2022).